PCCP

Accepted Manuscript

ROYAL SOCIETY OF CHEMISTRY

www.rsc.org/pccp

Journal Name

RSCPublishing

ARTICLE

Investigation of the interaction between novel unnatural chiral ligand and reactant on palladium for asymmetric hydrogenation

Cite this: DOI: 10.1039/xoxxoooooox

Received ooth January 2012,
Accepted ooth January 2012

DOI: 10.1039/xoxxoooooox

www.rsc.org/

Eun Hee Jeon,[a] Sena Yang,[a] Sung Ho Kang,[a] Sehun Kim [a] and Hangil Lee[*b]*

We report that mechanistic studies of the reaction between a newly synthesized (*S*)-2-((*R*)-3*H*-dinaphtho[2,1-*c*:1',2'-*e*]azepin-4(5*H*)-yl)-2-phenylethanol based on the binaphthyl skeleton and (*E*)-2-methyl-5-phenylpent-2-enoic acid for the asymmetric hydrogenation of *α, β* - unsaturated acids with heterogeneous palladium catalysts. The specific interactions between the chiral ligand and reactant were investigated in solution with palladium nanoparticles, as well as under ultrahigh vacuum (UHV) conditions on the palladium metal surface in the absence of hydrogen. The reactions were explored using nuclear magnetic resonance (NMR) spectroscopy, scanning tunneling microscopy (STM), and high-resolution photoemission spectroscopy (HRPES) combined with density functional theory (DFT) calculations. NMR study identified the interaction between both molecules with palladium nanoparticles in solution. In addition, STM and HRPES studies revealed the spatial distribution and configuration of both compounds on the palladium metal surface under UHV conditions. The theoretical results support the experimental results with respect to the interaction energy value. It was found that the reaction between the ligand and reactant occurs with the hydrogen bonding on palladium surface, simultaneously. The present study provides mechanistic details of the asymmetric hydrogenation reaction, which bears correlation between ligand, reactant, and catalyst during the reaction.

Introduction

The asymmetric heterogeneous hydrogenation over transition metal catalysts is a highly encouraging reaction process in industrial applications, such as for pharmaceuticals, agrochemicals, fragrances, and advanced materials defined by the significant chiral compounds include enantiomers.[1-3] Despite the growing interest in pure enantiomers, asymmetric reactions with heterogeneous catalysts are still limited in organic systhesis.[4] The studies with surface characterization techniques, spectroscopic analysis, and computational studies have been reported to better understand the heterogeneous asymmetric reaction mechanisms by chemists.[4] However, the mechanism of the asymmetric heterogeneous catalytic reactions was not clear, and the scope of reactions still remain narrow.[5]

According to the previous reports, significant catalytic systems has been achieved by the chiral modified catalyst, which is a fascinating research area and involves homogeneous transition-metal complexes combined with chiral molecules.[6-8] Various chiral modified catalyst systems have been used in the heterogeneous hydrogenation of C=C, C=N, and C=O bonds.[8,9] It has been investigated that three types of catalysts have been developed, such as the pyruvate over the platinum-cinchona system reported by Orito *et al*. (1979),[10] tartaric acid-modified nickel/NaBr,[11] and cinchona-modified palladium, described by Baiker *et al*. (1985).[12] In particular, platinum is well known catalysts for asymmetric hydrogenation because it provides selective hydrogenation of *α* – ketoesters reactants.[8,13] These mechanisms have been revealed by three different models: the adsorption model,[14] the shielding model,[15] and the zwitterion model.[16] This reaction mechanism of the platinum-cinchona system described by Orito *et al*. was explored using attenuated total reflectance-infrared (ATR-IR) spectroscopy and reflection adsorption infrared spectroscopy (RAIRS) techniques.[17-19] Evans's groups reported the adsorption of cinchona alkaloids on Pt using near edge X-ray absorption fine structure (NEXAFS),[20] and Raval's group examined the adsorption of tartaric acid on both Cu and Ni surfaces using RAIRS and NEXAFS techniques.[21,22] Particularly, one of the chiral ligand, naphthylethylamine, has been studied using NEXAFS, X-ray photoelectron spectroscopy (XPS), and STM techniques in order to study the adsorption and spatial distribution on Pt surface.[23,24] However, only a few groups have reported the palladium-catalyzed asymmetric reaction associated with chiral molecules-directed hydrogenation has been investigated.[25,26] To reveal the reaction mechanism for the palladium-catalyzed reactions, researchers utilized spectroscopic measurements, such as RAIRS,[28,30-32] XPS,[29] and STM.[27,32,33] In particular, the STM images are only available in the chiral ligand, cinchonidine, on Pd surfaces reported by Baiker *et al*,[34] and

theoretical studies were conducted to analyze the stable conforms of the chiral ligands on Pd surfaces.[35]

Thus, we focused on the hydrogenation of C=C bonds with modified chiral molecules on palladium catalysts, and also the correlation of chiral ligand and reactant on palladium surface because chiral-modified Pd catalyst offers effective C=C bond hydrogenation of *α, β* – unsaturated carboxylic acids compared to Ni and Pt, while the asymmetric hydrogenation on palladium catalysts have received much less attention than Pt catalysts in regard to the detailed mechanisms.[36] To investigated detailed reaction process of C=C bond hydrogenation using surface spectroscopic analysis, we engaged newly synthesized chiral ligand (*S*)-2-((*R*)-3*H*-dinaphtho[2,1-*c*:1',2'-*e*]azepin-4(5*H*)-yl)-2-phenylethanol (marked by chiral ligand **1** in Scheme 3) based on the binaphthyl skeleton containing a condensed aromatic ring, tertiary nitrogen and chiral center, which has a crucial characteristic of the efficient ligand like cinchonidine for the asymmetric heterogeneous hydrogenation reactions of C=C bonds. Although hydrogenations over the chiral ligand **1** show a low ee values (see the Supporting information Table S1), this chiral ligand **1** can help to identify the interaction between the chiral ligand and reactant on palladium surface using spectroscopic measurements. We have also developed the reactant (*E*)-2-methyl-5-phenylpent-2-enoic acid (marked by reactant **2** in Scheme 3) based on the *α, β* – unsaturated carboxylic acids, which is suitable compound for experiments.

In this paper, the specific interaction between the chiral ligand **1** and reactant **2** with palladium nanoparticles is carefully observed in atmospheric condition as well as under ultrahigh vacuum (UHV) conditions. We applied ex-situ NMR technique to investigate the interaction between the chiral ligand **1** and reactant **2** over 5% Pd/Al_2O_3 nanoparticles in solution. Moreover, STM and HRPES were applied to investigate the spatial distribution and adsorption configuration of chiral molecules using the single Pd(111) metal surface under UHV conditions. Finally, DFT calculations were utilized to obtain information about the stable condition and matched with experimental data.

Experimental

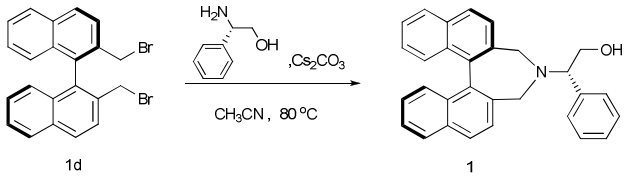

Scheme 1 Synthesis of (*S*)-2-((*R*)-3*H*-dinaphtho[2,1-*c*:1',2'-*e*]azepin-4(5*H*)-yl)-2-phenylethanol.

Procedure for synthesizing the chiral ligand 1.

(*R*)-2,2'-bis(bromomethyl)-1,1'-binaphthalene (**1d**) was synthesized according to the known literature procedures from commercially available (*R*)-1,1'-bi(2-naphthol) through 3 steps.[37] (Scheme 1) To a stirred solution of the compound (**1d**) (0.0886 mmol) in acetonitrile was added (*S*)-2-amino-2-phenylethanol (0.1772mmol) at 80 °C. Cs_2CO_3 (0.1772 mmol) was then added. The reaction mixture was stirred overnight and then treated with H_2O to quench. After 1 hour, the mixture was diluted with EtOAc and H_2O. It was extracted with EtOAc, followed by purification by column chromatography (EtOAc / Hexane = 1/2 (v/v)). The chiral ligand **1** was prepared from (*R*)-1,1'-bi(2-naphthol) in 67% overall yield. (Supporting information available in detail, Scheme S1)

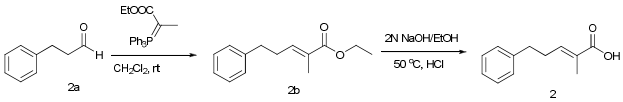

Scheme 2 Synthesis of ((*E*)-2-methyl-5-phenylpent-2-enoic acid).

Procedure for synthesizing the reactant 2.

To prepare the reactant **2**, ethyl 2-(triphenylphosphoranylidene)propanoate (1.52998 mmol) and 3-phenylpropanal (**2a**) (1.27498 mmol) were dissolved in CH_2Cl_2 at rt. After stirring for 4 hours, the mixture was quenched with aqueous NH_4Cl solution and extracted with CH_2Cl_2. Purification by flash column chromatography (Et_2O/Hexanc=1/50 (v/v)) furnished (*E*)-ethyl 2-methyl-5-phenylpent-2-enoate (**2b**) in 95% yield; this compound **2b** was then hydrolyzed (*E*)-2-methyl-5-phenylpent-2-enoic acid (**2**). (Scheme 2) The ester **2b** (1.204 mmol) was dissolved in 2 N NaOH/EtOH (60.217 mmol) at 50 °C and stirred for 2 hours. This resulting solution was acidified by addition of HCl solution and extracted with EtOAc. Column chromatography (Et_2O/Hexane=1/2 (v/v)) afforded the unsaturated acid **2** in 99% yield.[38] (Supporting information available in detail, Figure S1)

NMR experiments.

The ^{1}H-NMR spectra were recorded using an AVANCE 400 MHz spectrometer in chloroform-*d* as the common solvent and reported in parts per million from internal standard at ambient temperature. Each spectrum was recorded from the chiral ligand **1**, reactant **2**, and the complex of both molecules in the presence of 5% Pd/Al_2O_3 nanoparticles, to compare the peak shifts.

STM experiments.

The Pd(111) surface (9 mm diameter, 0.3 mm thick, R = 0.6 Ω) was cleaned by Ar^+ ions sputtering (1 keV), followed by heating to 1000 K in 3×10^{-8} Torr of oxygen, and then annealing at 1200 K in vacuo to remove any remaining oxygen.[27,28,32] STM experiments were conducted in an ultrahigh-vacuum (UHV) chamber equipped with an OMICRON VT-STM instrument at a base pressure below 2.0×10^{-10} Torr. All STM images were recorded using an electrochemically etched tungsten tip at a bias voltage of -2.0 V with a tunneling current of 0.1 nA. All images were collected from the synthesized chiral ligand **1** and reactant **2**. Following chiral ligand **1** dosing, images were acquired at ambient temperature, followed by dosing reactant **2** in sequence.

HRPES experiments.

HRPES measurements were conducted at the 10D beamline of the Pohang Accelerator Laboratory. The Pd 3*d*, C 1*s*, N 1*s*, and O 1*s* core-level spectra were obtained using a PHOIBOS 150 electron energy analyzer equipped with a two-dimensional charge-coupled device (2D CCD) detector (Specs GmbH). Photon energies of 400, 340, 460, and 590 eV were used to enhance the surface sensitivity. The binding energies of three core-level spectra were calibrated with respect to the energy of the clean Au 4*f* core-level spectrum (84.0 eV) at the same photon energy. The base pressure of the chamber was maintained below 9.5×10^{-11} Torr. All spectra were recorded in the normal emission mode. The photoemission spectra were carefully analyzed using a standard nonlinear least squares

fitting procedure with Voigt functions.[39] The Pd(111) surface was cleaned by repeatedly applying Ar^+ ions sputtering (1 keV), and annealing in 5×10^{-8} Torr of O_2 at 1000 K.[28,33]

Theoretical calculations.

The interactions that were expected to lead hydrogen bond formation on the Pd(111) surfaces were investigated by performing DFT calculations using the JAGUAR 9.1 software package employing a hybrid density functional method that included the Becke's three-parameter nonlocal exchange functional with the correlation functional of Lee–Yang–Parr (B3LYP).[40] DFT calculations were conducted to predict the stable energies of each molecule and expected interactions derived from experimental results between the chiral ligand **1** and reactant **2** on the palladium clusters. These calculations considered Pd_{96} cluster models with related to the periodic two-layer Pd slab were used to compute the stable energy.[41] The geometries of important local minima on the potential energy surface were determined at the B3LYP/LACVP** level of theory. The LACVP** basis set is a mixed basis set that uses the LACVP basis set to describe the Pd atoms and the 6-31G basis set for the remaining atoms. Moreover, the LACVP basis set describes atoms beyond Ar in the periodic table using the Los Alamos effective core potentials developed by Hay and Wadt.[42]

Results and discussion

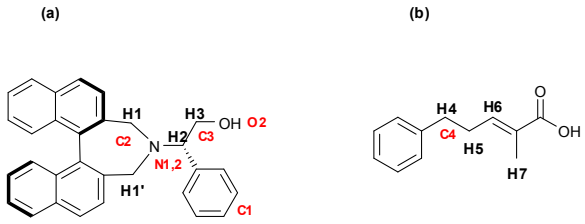

Scheme 3 The structures of (a) (*S*)-2-((*R*)-3*H*-dinaphtho[2,1-*c*:1',2'-*e*]azepin-4(5*H*)-yl)-2-phenylethanol (ligand **1**) and (b) (*E*)-2-methyl-5-phenylpent-2-enoic acid (reactant **2**). Letter color: NMR data (black), HRPES data (red).

We investigated detailed process of asymmetric heterogeneous hydrogenation reaction using chiral ligand **1** and reactant **2** in solution and then examined the adsorption configuration and the spatial distribution of the chiral ligand **1** under UHV conditions in the absence of hydrogen. Moreover, we examined the stable energy values of the individual molecules and the complexes were compared to corroborate experimental results.

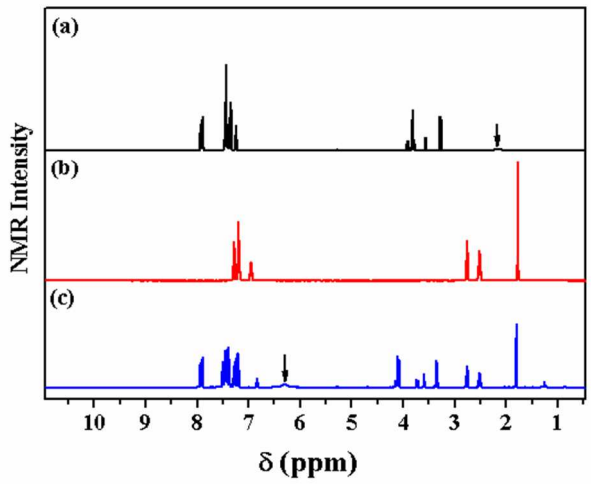

Fig. 1 ^{1}H NMR spectrum of the (a) ligand **1**, (b) reactant **2**, and (c) interaction between ligand **1** and reactant **2** with 5% Pd/Al_2O_3 (L/R = 1 mol% in chloroform-*d*).

Figure 1 indicates the assignment of the ^{1}H NMR spectrum for chiral ligand **1** and reactant **2** in chloroform-*d* (^{1}H NMR spectrum in methanol-d_4 available in Supporting information, see Figure S2). The H1 and H1' protons of the chiral ligand **1** shown in Figure 1a appear as two of doublets at δ 3.26 and 3.80, respectively, due to the long-range coupling between H1 or H1' and one of the ring protons.[37] The chiral center proton, H2, appears as a triplet at δ 3.56. The two protons of H3 appear as a quartet at δ 3.78 and 3.91, respectively. The O-H proton is associated with a broad signal at δ 2.16. Figure 1b shows the spectrum of the *α, β* – unsaturated acids, reactant **2**. The protons, H4 and H5 appear as a triplet at δ 2.76 and a quartet at δ 2.52, respectively. H6, which is easily identified by its NOESY with H5 and H7 (see the Supporting information Figure S1), appears as a triplet at δ 6.95. The COO-H proton is associated with a broad peak at δ 10.74.

The ^{1}H NMR spectrum of the mixture with the chiral ligand **1**, reactant **2** and Pd nanoparticles substantiated the existence of the interaction structure between both molecules, as shown in Figure 1c. A new peak was observed at δ 6.30. The intensity of the carboxyl COO-H peak measured by ATR-IR was decrease compared with its original intensity (Supporting information available in Figure S3). Williams *et al*. previously studied the interactions between the chiral ligand, cinchonidine, and reactant on the Pd(111) surface over the ATR-IR system.[43] An up-field shift in the *β* - proton on the *α, β* – unsaturated acids, reactant **2** at δ 6.83 relative to the original peak position at δ 6.95 (Figure 1b) was observed in the ^{1}H NMR spectrum due to the low basicity of the reactant.[44] The ^{1}H NMR peaks corresponding to H1, H1', H2, and H3 appear at more down-field positions (δ 3.35, 4.10, 3.59, and 3.73 with 4.14, respectively).[45]

Here, the chiral ligand **1** acts as an electron donor, whereas reactant **2** acts as an electron acceptor during the reaction in the absence of hydrogen. We suppose that this peak shifts resulted from the acid-base complexes that formed between the nitrogen on the chiral ligand 1 and the acidic proton on reactant 2.[46] The ^{1}H NMR results indicate that there is the interaction between the chiral ligand **1** and reactant **2**.[47-49]

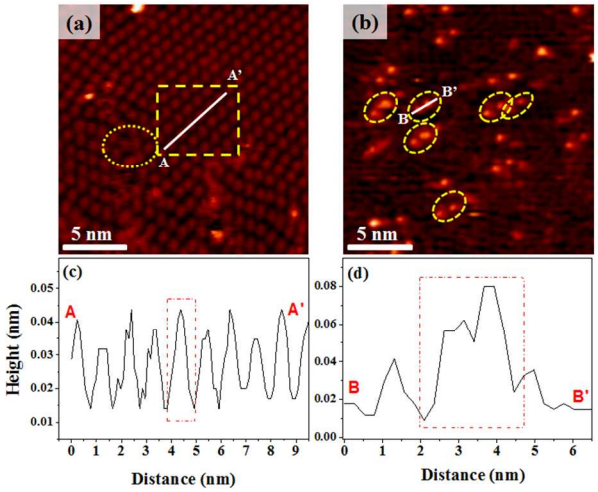

Fig. 2 STM images of the (a) chiral ligand **1** on the Pd(111) surface at low coverage taken at ambient temperature (20 × 20 nm), (b) both molecules (ligand **1** and reactant **2**) formed complexes on the Pd(111) surface (20 × 20 nm). V_b = -2.0 V, I_t = 0.1 nA. The line profiles along the white lines are shown on the bottom; (c) the individual chiral ligand **1**, (d) the complexes.

The spatial distribution of the individual ligand **1** and complexes following exposure to reactant **2** in sequence on the Pd(111) surface under UHV conditions in the absence of hydrogen, was examined using scanning tunneling microscopy (STM). Figure 2a shows the image of the individual chiral ligand **1**. Complexes of both molecules on the clean Pd(111) surface are shown in Figure 2b.[50] Each molecule of the chiral ligand **1** appears as small uniform balls with about size 1.1 nm, as shown in the line profile A-A' in Figure 2c. One region shows well-ordered domains (marked by the square box in Figure 2a) resulting from inter-molecular interactions of the chiral ligands **1**, and another is the disordered region (marked by the circle in Figure 2a) with non-intermolecular interactions among the chiral ligand **1** along different directions.[51] It should be noted that a distinct boundary with a disordered region is present. The non-interacting individual chiral ligand **1** molecules in the disordered region were sufficiently isolated that reactant **2** molecules could approach when after dosing the reactant **2**.

After scanning the STM image of the chiral ligand **1** on the Pd(111) surfaces (Figure 1a), dosing of the reactant **2** molecules proceeded in sequence. Figure 2b shows the images of the complexes between both molecules with two little asymmetric neighboring circular shapes (marked by the oval), while with no changes in the well-ordered domains. The STM images of the wide range with the ordered domains are displayed in supporting information, Figure S4. The appearance of the yellow dot ovals indicates interactions between two neighboring circles of the chiral ligand **1** and reactant **2**, rather than interactions between chiral ligands **1**. This interaction was revealed through the measured apparent distance and height profiles shown in Figure 2d. The line profiles along the traces B-B' show the complex between the chiral ligand **1** and reactant **2** with about 2 nm long. Interactions between both molecules occurred selectively at the boundaries in the disordered region where the well-ordered domains oriented along different directions. (Figure 2b)

The selectivity of this interaction depends on the localized accessibility of reactant **2** to the chiral ligand **1** due to the wide spatial distribution within the disordered region. These results indicated that the distribution of the chiral ligand **1** on the Pd(111) surface affects the interaction with the reactant **2**. The STM images show the presence of the inter-molecular interactions among the chiral ligands **1** in the well-ordered region, and provide evidence for the 1:1 interaction model between the chiral ligand **1** and reactant **2** in the disordered region, based on the distance changes measured in the line profile.[52]

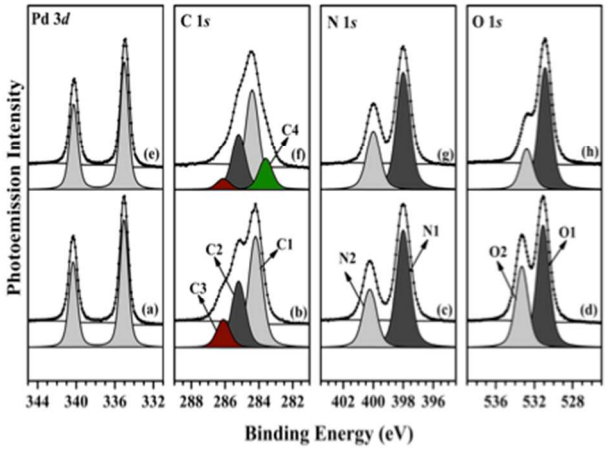

Fig. 3 Pd 3*d*, C 1*s*, N 1*s*, and O 1*s* core-level spectra for (a, b, c, d) ligand **1** adsorbed and for (e, f, g, h) ligand **1** with reactant **2** on the Pd(111) surface. The dots indicate experimental values and the solid lines represent the results of peak fits.

The core-level spectra of Pd 3*d*, C 1*s*, N 1*s*, and O 1*s* were acquired following exposure of the chiral ligand **1** and reactant **2**, in sequence, on the clean Pd(111) surface to identify the distinct electronic structures of the interactions between the chiral ligand **1** and reactant **2** in absence of the hydrogen, as shown in Figure 3.

The Pd 3*d* core-level spectrum of the only chiral ligand **1** shows two peaks at 335 eV and 340 eV, in agreement with the spectrum obtained from reactant **2** in the presence of chiral ligand **1**, as shown in Figures 3a and e.[53] Owing to no variation differences, we revealed that the Pd metal is not involved in the initial interaction both molecules directly. In the presence of hydrogen, the Pd metal surface works as the catalyst through the Pd-H as the hydrogen suppliers.[54] The carbon 1*s* core-level spectrum of the chiral ligand **1** displays three peaks at 284.0 eV(C1), 285.2 eV(C2), and 286.1 eV(C3), associated with the $C_{C=C}$ (phenyl), C_{C-N} (tertiary amine), and C_{C-OH} (alcohol) groups, respectively (Figure 3b).[55] A new peak is observed at 283.6 eV (C4) corresponding to the C_{C-C} group (alkyl chain, sp^3) of reactant **2**. The binding energy of (C3) in the presence of the reactant **2**, as shown in Figure 3f, shows the low intensity of the peak corresponded to the presence of interactions between the chiral ligand **1** (C-OH) and the reactant **2** (COO-H), as expected.[50] Figures 3c and g show the N 1*s* core-level spectrum acquired at 398.1 eV (tertiary amine C-N, labeled N1) and 400.3 eV (protonated C-$^+$NH, labeled N2).[56] The (N2) peak position shifts toward lower binding energy slightly, as shown in Figure 3g. The O 1*s* core-level spectrum shown in Figure 3d indicates two components corresponding to two different types of oxygen atoms. The O 1*s* spectrum reveals binding energies of 531.1 eV (O1) and 533.2 eV (O2) relative to the alcohol group (-OH), as shown in Figure 3d.[57,58] According to the

previous results, the STM images of the individual chiral ligand **1** suggested that the (O1) peak generated as a result of the inter-molecular interactions among the chiral ligands **1** represented well-ordered regions within which the chiral ligand **1** did not interact with the reactant **2**. After exposure to reactant **2** in sequence, the intensity of the (O2) binding energy was lower than the initial intensity, and the (O1) peak position did not shift. (Figure 3h)

Our HRPES results indicate that both the oxygen atom in the alcohol and the nitrogen atom of the tertiary amine of the chiral ligand **1** participate in the interactions on the Pd(111) surface. Consequently, the peak shifts and the binding energy intensities indicate that the hydrogen bonding intermolecular interactions between the chiral ligand **1** and reactant **2** occurs at the specific positions in the disordered regions, consistent with the shifts observed for $^{+}$N-H….$^{-}$OC=O and O-H….O=CO- and the inter-molecular interactions among the chiral ligands **1** occurs in the well-ordered regions. This HRPES results are matched with NMR and STM experimental data on the specific interaction site.

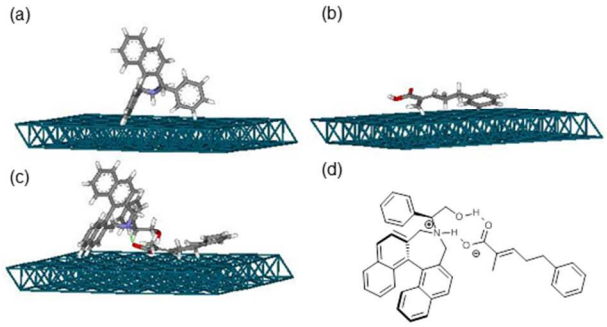

Fig. 4 Side view of the (a) chiral ligand **1** (E_{ad} = -35.75 kcal/mol), (b) reactant **2** (E_{ad} = -17.11 kcal/mol), and (c) structures of the complex (E_{ad} = -35.78 kcal/mol) on Pd(111) surface, calculated using DFT methods, and (d) schematic diagram of the complex. Atomic color codes: Pd (green), O (red), N (violet), C (gray), H (white).

The proposed adsorption stability of the complexes via hydrogen bonds between the chiral ligand **1** and reactant **2** was calculated using DFT calculation methods in the gas-phase. The calculated geometries of the chiral ligand **1**, reactant **2**, and the proposed complex geometry of both molecules, as shown in Figure 4, indicate the adsorption energy value. The energetically most stable adsorption geometry is calculated to be the complexes via hydrogen bonds with an adsorption energy of -35.78 kcal/mol. Figure 4d shows the proposed Schematic diagram between chiral ligand **1** and substrate **2** involving hydrogen bonds, from above assuming the metal surface being below presenting the O-H group of the chiral ligand **1** bound to the carbonyl oxygen (-C=O) of reactant **2**, and the protonated amine (-$^{+}$N-H) of the chiral ligand **1** bound to the deprotonated carboxylate anion (-O-C=O), in agreement with the previous experimental observations. Note that the structure shown in Figure 4c, which contained hydrogen bonds, was found to be more stable than the structures of the individual molecules.

Conclusions

We have revealed detailed process of the palladium-catalyzed for the asymmetric heterogeneous hydrogenation of C=C bonds using the newly synthesized chiral binaphthol ligand **1** and reactant **2**. The experimental data (NMR, STM, HRPES) and theoretical results (DFT calculations) led us to propose that the reaction proceeds via a hydrogen bonding interaction both in solution and under UHV conditions. NMR experiments suggested that the interaction between the nitrogen on chiral ligand **1** and acidic proton on reactant **2** in solution with palladium nanoparticles, based on the observed peak shift. The STM data demonstrated that the spatial distribution of individual chiral ligands **1** and the selective formation of complexes depends on the ordering of the chiral ligand **1** on the Pd(111) surface under UHV conditions. We believe that the spatial distribution of the chiral ligand is an important factor for the interaction between both molecules. Moreover, the HRPES data revealed the electronic structures of the interactions between the chiral ligand **1** and the reactant **2**, and validated the structures of the inter-molecular interactions in only well-ordered regions among the chiral ligands **1** compared to previous STM results, which examined well-ordered and disordered regions. The hydrogen bonds associated with the interactions were calculated to be energetically feasible through the DFT calculations. We also provided that the reaction scope of the palladium-catalyzed asymmetric reaction expands with the newly synthesized chiral binaphthol ligand **1** and reactant **2**.

Acknowledgements

This research was supported by the National Research Foundation of Korea (NRF) with funding from the Korea government (MSIP) (No. 20090083525 and No. 2015021156).

Notes and references

[a] *Molecular-Level Interface Research Center, Department of Chemistry, KAIST, Daejeon 305-701, Republic of Korea.*

[b] *Department of Chemistry, Sookmyung Women's University, Seoul 140-742, Republic of Korea. E-mail: easyscan@sookmyung.ac.kr*

† Electronic Supplementary Information (ESI) available: Detailed experimental procedures and characterization data obtained from the prepared compounds. See DOI: 10.1039/b000000x/

1 (*a*) W. A. Nugent, T. V. RajanBabu and M. J. Burk, *Science,* 1993, **259**, 479-483; (*b*) P. Kraft, J. A. Bajgrowicz, C. Denis and G. Frater, *Angew. Chem. Int. Ed.,* 2000, **39**, 2980-3010; (*c*) H. U. Blaser, F. Spindler and M. Studer, *Appl. Catal. A: Gen*., 2001, **221**, 119-143.

2 R. Noyori, *Angew. Chem. Int. Ed.,* 2002, **41**, 2008-2022.

3 O. Deutschmann, in *Heterogeneous Catalysis and Solid Catalysts,* ed. H. Knozinger, K. Kochloefl and T. Turek, Wiley-VCH, Weinheim, 2009, pp. 1-110.

4 Z. Wang in *An overview of Heterogeneous Asymmetric Catalysis*, ed. K. Ding and Y. Uozumi, Wiley-VCH, Weinheim, 2008, pp. 1-24.

5 E. Zhan, C. Chen, Y. Li and W. Shen, *Chem. Soc. Rev.,* 2014, DOI: 10.1039/c4cy00900b.

6 M. Heitbaum, F. Glorius and I. Escher, *Angew. Chem. Int. Ed.,* 2006, **45**, 4732-4762.

7 M. Studer, H. U. Blaser and C. Exner, *Adv. Synth. Catal.,* 2003, **345**, 45-65.

8 A. Baiker, *J. Mol. Catal. A: Chem.,* 1997, **115**, 473-493.

9 M. Bartok, G. Wittmann, G. Gondos and G. V. Smith, *J. Org. Chem*., 1987, **52**, 1139-1141.
10 Y. Orito, S. Imai and S. Niwa, *Bull. Chem. Soc. Jpn.,* 1979, **52**, 1118.
11 Y. Izumi, M. Imaida, H. Fukawa and S. Akabori, *Bull. Chem. Soc. Jpn.,* 1963, **36**, 21-25.
12 W. -R. Huck, T. Mallat and A. Baiker, *J. Catal.,* 2000, **193**, 1-4.
13 Z. Ma, I. Lee, J. Kubota and F. Zaera, *J. Mo. Catal. A: Chem.,* 2004, **216**, 199-207.
14 O. Schwalm, B. Minder, J. Weber and A. Baiker, *Catal. Lett*., 1994, **23**, 271-279.
15 J. L. Margitfalvi, M. Hegedus and E. Tfirst, *Tetrahedron: Asymmetry,* 1996, **7**, 571-580.
16 G. Vayner, K. N. Houk and Y. -K. Sun, *J. Am. Chem. Soc.,* 2004, **126**, 199-203.
17 N. Bonalumi, T. Burgi and A. Baiker, *J. Am. Chem. Soc.,* 2003, **125**, 13342-13343.
18 D. Ferri and T. Burgi, *J. Am. Chem. Soc.,* 2001, **123**, 12074-12084.
19 S. Lavoie, M. -A. Laliberte and P. H. McBreen, *J. Am. Chem. Soc.,* 2003, **125**, 15756-15757.
20 T. Evans, A. P. Woodhead, A. Gutiérrez-Sosa, G. Thornton, T. J. Hall, A. A. Davis, N. A. Young, P. B. Wells, R. J. Oldman, O. Plashkevych, O. Vahtras, H. Ågren and V. Carravetta, *Surf. Sci.,*1999, **436**, L691-L696.
21 M. Castonguay, J. -R. Roy, A. Rochefort and P. H. McBreen, *J. Am. Chem. Soc.,* 2000, **122**, 518-524.
22 S. M. Barlow and R. Raval, *Surf. Sci. Rep.,* 2003, **50**, 201-341.
23 J. M. Bonello, E. C. H. Sykes, R. Lindsay, F. J. Williams, A. K. Santra and R. M. Lambert, *Surf. Sci.,* 2001, **482-485**, 207-214.
24 (*a*) J. M. Bonello, F. J. Williams and R. M. Lambert, *J. Am. Chem. Soc.,* 2003, **125**, 2723-2729; (*b*) A. D. Gordon and F. Zaera, *Angew. Chem. Int. Ed.,* 2013, **52**, 3453-3456.
25 S. K. Beaumont, G. Kyriakou, D. J. Watson, O. P. H. Vaughan, A. C. Papageorgiou and R. M. Lambert, *J. Phys. Chem. C*, 2010, **114**, 15075-15077.
26 A. Tungler, M. Kajtar, T. Ma´the´, G. Toth, E. Fogassy and J. Petro´, *Catal. Today,* 1989, **5**, 159-171.
27 S. Katano, H. S. Kato, M. Kawai and K. Domen, *J. Phys. Chem. C,* 2009, **113**, 14872-14878.
28 F. Calaza, D. Stacchiola, M. Neurock and W. T. Tysoe, *Surf. Sci.*, 2005, **598**, 263-275.
29 J. M. Bonello, R. Lindsay, A. K. Santra and R. M. Lambert, *J. Phys. Chem. B,* 2002, **106**, 2672-2679.
30 W. Chu, R. J. LeBlanc, C. T. Williams, J. Kubota and F. Zaera, *J. Phys. Chem. B*, 2003, **107**, 14365-14373.
31 L. Burkholder and W. T. Tysoe, *J. Phys. Chem. C,* 2009, **113**, 15298-15306.
32 L. Burkholder, D. Stacchiola, J. A. Boscoboinik and W. T. Tysoe, *J. Phys. Chem. C,* 2009, **113**, 13877-13885.
33 J. A. Boscoboinik, Y. Bai, L. Burkholder and W. T. Tysoe, *J. Phys. Chem. C,* 2011, **115**, 16488-16494.
34 (*a*) M. Wahl, M. von Arx, T.A. Jung and A. Baiker, *J. Phys. Chem. B,* 2006, **110**, 21777-21782; (*b*) M. von Arx, M. Wahl, T.A. Jung and A. Baiker, *Phys. Chem. Chem. Phys.,* 2005, **7**, 273-277.
35 E. Schmidt, C. Bucher, G. Santarossa, T. Mallet, R. Gilmour and A. Baiker, *J. Catal.* 2012, **289**, 238-248.
36 S. Tan, J. R. Monnier and C. T. Williams, *Top. Catal.,* 2012, **55**, 512-517.
37 T. Ooi, M. Kameda and K. Maruoka, *J. Am. Chem. Soc*., 2003, **125**, 5139-5151.
38 C. C. Browder, F. P. Marmsater and F. G. West, *Can. J. Chem.,* 2004, **82**, 375-385.
39 F. Schreier, *J. Quant. Spectrosc. Radiat. Transfer,* 1992, **48**, 743-762.
40 W. Kohn, A. D. Becke and R. G. Parr, *J. Phys. Chem.,* 1996, **100**, 12974-12980.
41 M. Neurock and R. A. van Santen, *J. Phys. Chem. B,* 2000, **104**, 11127-11145.
42 P. J. Hay and W. R. Wadt, *J. Chem. Phys.,* 1985, **82**, 299-310.
43 S. Tan and C. T. Williams, *J. Phys. Chem. C,* 2013, **117**, 18043-18052.
44 (*a*) G. N. LaMar, T. J. Bold and J. D. Satterlee, *Biochim. Biophys. Acta,* 1977, **498**, 189-207; (*b*) J. Y. Kim, S. M. Park and H. -S. So, *Bull. Korean Chem. Soc*., 1997, **18**, 369-373.
45 S. R. Chaudhari and N. Suryaprakash, *J. Mol. Struct.* 2012, **1016**, 163-168.
46 P. Lorente, I. G. Shenderovich, N. S. Golubev, G. S. Denisov, G. Buntkowsky and H. -H. Limbach, *Magn. Reson. Chem.* 2001, **39**, S18-S29.
47 R. L. Mills, J. He, M. Nansteel and B. Dhandapani, *Int. J. Global Energy,* 2007, **28**, 304-324.
48 W. -R. Huck, T. Burgi, T. Mallat and A. Baker, *J. Catal.*, 2001, **200**, 171-180.
49 W. -R. Huck, T. Burgi, T. Mallat and A. Baker, *J. Catal*., 2003, **219**, 41-51.
50 Y. -G. Kim, J. H. Baricuatro, M. P. Soriaga and D. W. Suggs, *J. Electroanal. Chem.,* 2001, **509**, 170-174.
51 C. Stadler, S. Hansen, I. Kroger, C. Kumpf and E. Umbach, *Nat. phys.,* 2009, **5**, 153-158.
52 (*a*) B. -I. Kim, C. Cai, X. Deng and S. S. Perry, *Surf. Sci.* 2003, **38**, 45-52; (*b*) J. Weckesser, J. V. Barth and K. Kern, *J. Chem. Phys.,* 1999, **110**, 5351-5354.
53 E. H. Voogt, A. J. M. Mens, O. L. J. Gijzeman and J. W. Geus, *Surf. Sci.,* 1996, **350**, 21-31.
54 (*a*) D. Teschner1, A. Pestryakov, E. Kleimenov, M. Hävecker, H. Bluhm, H. Sauer, A. Knop-Gericke and R. Schlögl, *J.Catal.,* 2005, **230**, 186-194; (*b*) M. Armbrüster, M. Behrens, F. Cinquini, K. Fçttinger and Y. Grin, *et al*. *ChemCatChem* 2012, **4**, 1048-1063.
55 E. A. Hoffmann, T. Kortve´lyesi, E. Wilusz, L. S. Korugic-Karasz, F. E. Karasz and Z. A. Fekete, *J. Mol. Struct.: THEOCHEM,* 2005, **725**, 5-8.
56 W. J. Gammon, O. Kraft, A. C. Reilly and B. C. Holloway, *Carbon* 2003, **41**, 1917-1923.
57 D. Rosenthal, M. Ruta, R. Schlögl and L. Kiwi-Minsker, *Carbon,* 2010, **48**, 1835-1843.
58 S. Kundu, Y. Wang, W. Xia and M. Muhler, *J. Phys. Chem. C,* 2008, **112**, 16869-16878.

